TÜBİTAK

Turkish Journal of Earth Sciences

http://journals.tubitak.gov.tr/earth/

Research Article

Turkish J Earth Sci
(2015) 24: 494-512

doi:10.3906/yer-1407-12

Estimating depth to the bottom of magnetic sources at Wikki Warm Spring region, northeastern Nigeria, using fractal distribution of sources approach

Ema Michael ABRAHAM[1,*], Ene Grace OBANDE[2], Mbazor CHUKWU[3], Chibuzo Gabriel CHUKWU[1], Mkpuma Rock ONWE[4]

[1]Department of Geophysics, Federal University Ndufu Alike Ikwo, Ebonyi State, Nigeria
[2]Department of Quality Assurance, National University Commission, Abuja, Nigeria
[3]Department of Civil Engineering, Federal University Ndufu Alike Ikwo, Ebonyi State, Nigeria
[4]Department of Geology, Federal University Ndufu Alike Ikwo, Ebonyi State, Nigeria

Received: 14.07.2014 • **Accepted/Published Online:** 13.04.2015 • **Printed:** 04.09.2015

Abstract: The Wikki Warm Spring (WWS) is located on the Kerri-Kerri formation of tertiary age. This forms part of the Benue Basin, which links up with the Chad Basin in the north and extends southwest to the Anambra Basin in Nigeria. The stratigraphy of the WWS region consists of alluvium, the Kerri-Kerri formation, the Gombe formation, the Pindiga formation, the Yolde formation, the Bima formation, and basement rocks as the oldest. We estimate the depth to the bottom of magnetic sources (DBMS) in the WWS region using the fractal sources distribution approach on aeromagnetic data to identify the geothermal system of the WWS region. The adopted computational method is based on statistical methods of depth determination from the radial power spectrum assuming a fractal distribution of magnetic sources. The average estimated DBMS at the WWS source location is 10.72 ± 0.54 km. The obtained results imply an average thermal gradient of 54.11 °C km^{-1} and heat flow value of 135.28 mW/m^2. Generally, shallow DBMS values are obtained in the northeastern region of the WWS area and these increase towards the southwestern region when regional variation patterns of estimated depths are considered. The generally shallow DBMS obtained in the study area is attributed to magmatic intrusion or diapirism in the subsurface and emphasizes the effects of large-scale tectonic events, particularly the basin-initiating event, as major influences on the thermal history. Results will contribute to decisions on where to drill boreholes for further geothermal energy exploration in the region.

Key words: Aeromagnetic data, spectral analysis, fractals, Curie point depth, Wikki Warm Spring

1. Introduction

Proper estimation of depth to the bottom of magnetic sources (DBMS) around the Wikki Warm Spring (WWS) region could provide information about the thermal structure of the crust in the region. However, such studies are lacking at present. Because the basal depths of the magnetic sources can also be caused by contrasts in lithology rather than by temperatures in the crust above the Curie point, the DBMS does not necessarily coincide with the Curie temperature depth in detail (Bansal et al., 2011). In many studies (e.g., Tanaka et al., 1999; Trifonova et al., 2009; Bansal et al., 2011; Abraham et al., 2014), the DBMS is used as an estimate of the Curie point depth (CPD) and therefore as a proxy for temperature at depth. The CPD is the depth at which rocks lose their ferromagnetic magnetization as a result of an increase of the temperature in the crust above the Curie temperature. In spite of the limitations, the DBMS/Curie depth can be used to complement geothermal data in regions where deep boreholes are unavailable (Ross et al., 2006; Bansal et al., 2011; Abraham et al., 2014).

The WWS is located at 9.75°N, 10.5°E in Bauchi State within the study area (Figure 1). Using gravity data obtained from the middle Benue Trough, Ajayi and Ajakaiye (1981) provided explanations about the origin of the Benue Trough. Their results indicated the existence of a rift of about 40 km, buried under the Cretaceous cover, between the ridge of the trough and its northern boundary. From results of gravity measurements along two profiles in the Upper Benue Trough, broad negative anomalies characteristic of valleys with sedimentary fills were revealed with thickness of sediments in the survey area ranging between 1.0 km and 2.2 km (Osazuwa et al., 1981). Nur et al. (1999) estimated the CPD of the Upper Benue Trough to be between 23.80 and 28.70 km. They also obtained a depth of 0.83 km as the depth to magnetic sources and

* Correspondence: ema.abraham@funai.edu.ng

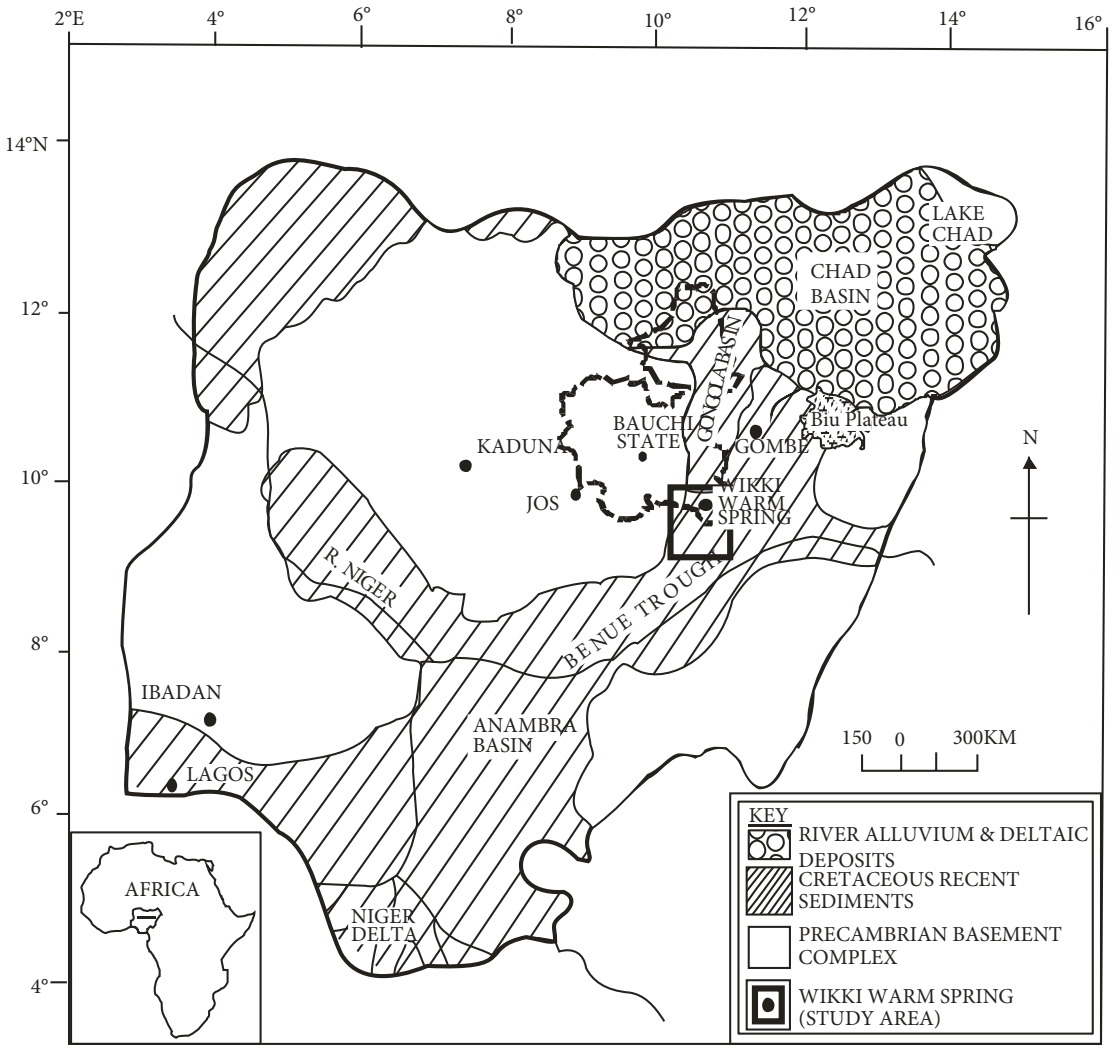

Figure 1. Location of Wikki Warm Spring on the Benue Trough of Nigeria. The dominant geology of Nigeria made mainly by crystalline (Precambrian Basement Complex) and sedimentary rocks (Cretaceous Recent Sediments) is also represented. The map also shows the location of Ikogosi town where the Ikogosi Warm Spring is located.

concluded that this depth represented the intrusive bodies within the trough. Radiometric survey of the WWS region (Omanga et al., 2001) revealed high gamma activity leading to the conclusion of possible radioactivity being the source of heat for the spring. Nwankwo et al. (2009) analyzed and interpreted wireline logs from 14 oil wells from the Nigerian sector of the Chad Basin (Figure 1) to estimate the heat flow trend in the basin. They computed geothermal gradients from corrected bottom hole temperatures obtained from gamma ray, resistivity, and sonic logs from the wells. Results from their heat flow calculations show a variation between 63.6 and 105.6 mW/m^2, with an average value of 80.6 mW/m^2. The Chad Basin developed at the intersection of many rifts, mainly in an extension of the Benue Trough (Nwankwo et al., 2009). Nine aeromagnetic maps were analyzed to determine some characteristics of a prominent aeromagnetic anomaly within the Gongola Basin in the Upper Benue Trough, northeastern Nigeria, by Abubakar et al. (2010). They assumed three magnetic layers in the area and computed average depth values of 1.25 km, 4.03 km, and 5.39 km for the layers, respectively. The depths to the causative body were determined as 2.40 and 8.09 km and the causative bodies were interpreted as basic and ultrabasic rocks. Kurowska and Schoeneich (2010) compiled a map of geothermal gradient for parts of the Chad Basin (extending towards our study area) from thermal data collected during pumping tests in water wells and several deep oil wells and presented a geothermal gradient map showing a general increase from 1.1 °C/m to 58 °C/m. Eletta and Udensi (2012) investigated the CPD

from magnetic data in the Benue Trough. Their area of investigation lay between 7°N and 9°30´N and between 9°30'E and 12°E. Their study area cuts our study area in half toward the southern region and lies within the sedimentary formation of the middle Benue Trough and partly in the basement complex region of north-central Nigeria. Their estimated CPDs varied between 2 to 8.4 km. Kasidi and Nur (2012) computed CPDs from aeromagnetic data over Sarti in northeastern Nigeria located at 7°N–8°N and 10°E–12°E (1° below our study area). They obtained CPDs between 26 to 28 km. Onuba et al. (2012) interpreted aeromagnetic data over parts of the Upper Benue Trough and southern Chad Basin within latitudes of 10°30´N to 11°30´N and longitudes of 12°E to 13°E (above our study area). They obtained depths to magnetic sources ranging from 0.5 to 2.5 km and concluded that the estimated depths were representative of the sedimentary thicknesses and intrusive bodies within the area. Alagbe and Sunmonu (2014) conducted evaluations on aeromagnetic data from the Upper Benue Trough within latitudes of 7°N to 8°N and longitudes of 11°E to 12°E (below our study area by a 1°N interval). Their estimated depth to the magnetic sources ranged between 0.01 and 3.45 km. They attributed the shallow depths to near-surface intrusive rocks in their study area.

Obande et al. (2014) attempted to investigate the geothermal potential of the WWS area using aeromagnetic data. They applied the spectral method to determine the depths to the top and centroid of magnetic sources in the study area. The power spectrum of magnetic anomalies was used to estimate the basal depth of the magnetic sources. Their results showed an average estimated CPD of 8 km and geothermal gradient of 68 °C/km with heat flow values averaging 170 mW/m^2.

In this study, we compute the DBMS using aeromagnetic data assuming a fractal distribution of magnetic sources to identify the geothermal system of the WWS region. Crustal magnetization is not completely uncorrelated but follows a fractal spatial distribution (Gregotski et al., 1991; Pilkington and Todoeschuck, 1993; Fedi et al., 1997; Maus et al., 1997; Li et al., 2013). The ultimate aim is to determine the DBMS with minimal uncertainty, to make geological and tectonic interpretations using the relation between DBMS and CPD, and to estimate the average surface heat flow of the WWS region.

1.1. Tectonic setting

The WWS lies within the Upper Benue Trough (Figure 1), a geological framework that was form during the Early Cretaceous rifting of the central West African basement uplift. It forms a regional structure that is exposed from the northern frame of the Niger Delta and runs northeastwards for about 1000 km to underneath Lake Chad, where it terminates (Eletta and Udensi, 2012). The West African Rift provides a unique example of a rift system interrupted in the course of its development and allows us to examine the effects of the underlying thermal disturbance in isolation from the rifting that produced it (Fitton, 1981). The formation of the Benue Trough is closely related with the transform zone that characterized the northern margin of the Gulf of Guinea during the early Cretaceous time of the continental separation between Africa and South America and the opening of the South Atlantic Ocean. The alignment of the West African Rift system is oriented mainly in a NE–SW direction (Burke and Whiteman, 1970; Freeth, 1982). This rift system may have been initiated and its course governed by hot spots, but most probably it evolved through stretching of the lithosphere in the areas around and between these hot spots (Fitton, 1981). The late Cretaceous evolution of the region is marked by a widespread event during the Santonian, being the consequence of the reorganization of plate motions (Benkhelil et al., 1989). An inevitable consequence of this stretching would be the development of linear zones where hot asthenosphere welled up passively into the lithosphere. The resulting thermal disturbance would extend down into the asthenosphere and at this point a geological accident decoupled the rift system from the deeper portions of this thermal disturbance and brought it to rest beneath what is now Cameroon. This disturbance then asserted itself in an active role and rose into the overlying lithosphere. In this way, an image of the Benue Trough thermal disturbance has been imprinted on the lithosphere beneath Cameroon and its magmatic effects are still being felt today (Fitton, 1981). The remarkable similarity in shape between the Benue Trough and the volcanic Cameroon line suggest that they are related to a common Y-shaped hot zone in the asthenosphere over which the African plate has moved (Fitton, 1980). Most deposits associated with the major sedimentary cycle in the Benue Trough (Figure 2) are believed to have been eroded as a result of a Late Cretaceous tectonic activity in the Upper Benue Trough (Kogbe, 1983; Nwachukwu, 1985). Aeromagnetic anomalies suggest that a series of buried NE–SW lineaments of incipient rifts controlled the deposition of the individual complexes (Eletta and Udensi, 2012). Benkhelil et al. (1989) suggested that the evolution of the trough could be a result of tension resulting in a rift or wrench-related fault basin. Mesozoic to Cenozoic magmatism accompanied the evolution of the tectonic rift as it is scattered all over and throughout in the trough (Coulon et al., 1996; Abubakar et al., 2010). The stratigraphy of the study area consists of alluvium, the Kerri-Kerri Formation, the Gombe Formation, the Pindiga Formation, the Yolde Formation, the Bima Formation, and basement rocks as the oldest (Figure 3).

The entire WWS is located on the Kerri-Kerri Formation of Tertiary age. This forms part of the Benue Basin, which

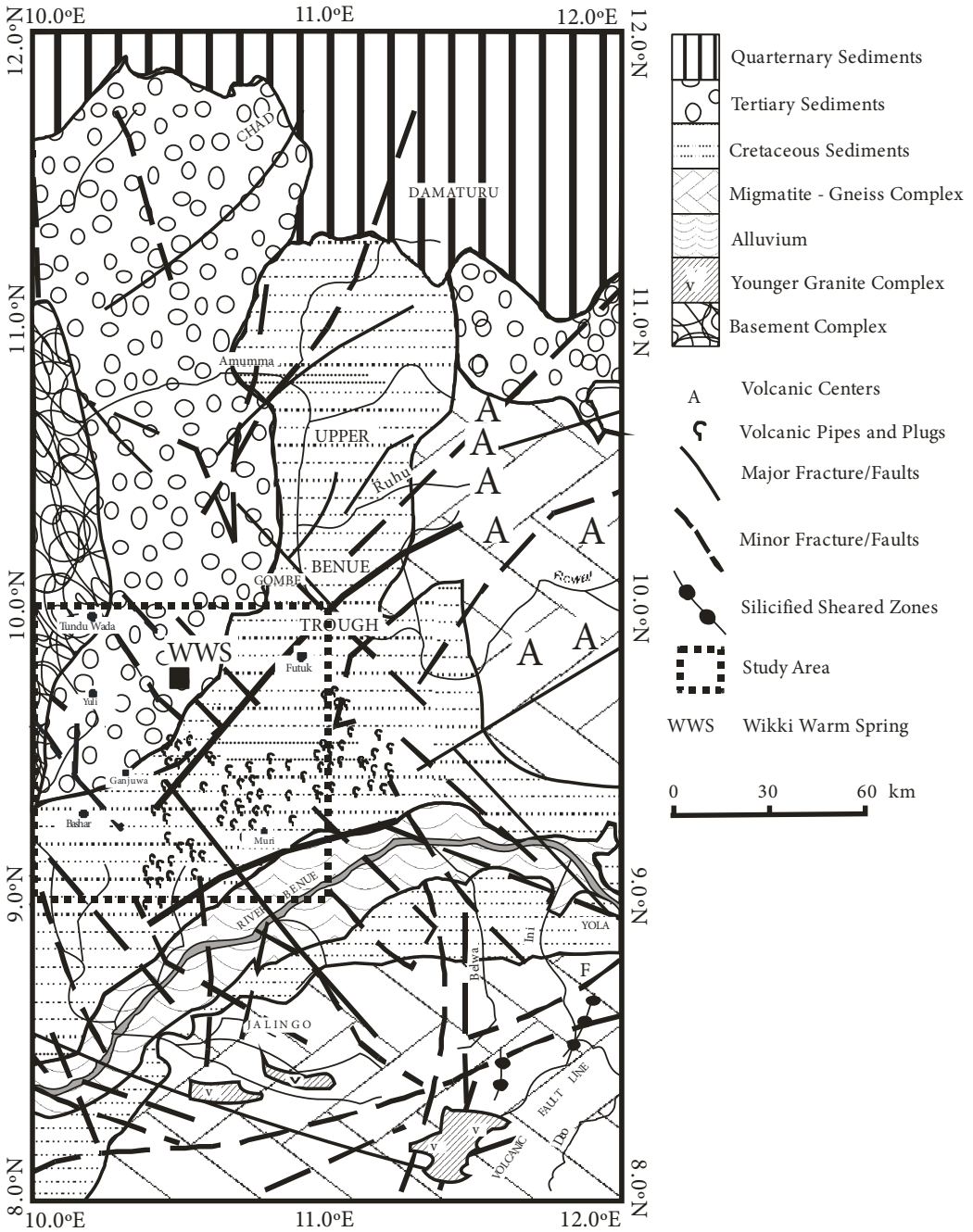

Figure 2. Tectonic setting of the WWS region.

links up with the Chad Basin in the north and extends southwest to the Anambra Basin (Obande et al., 2014). The Kerri-Kerri Formation was laid down in a continental environment ranging from lacustrine to deltaic, being derived from the weathering of the basement rocks as well as Cretaceous sedimentary formations. It outcrops in the northern part of the study area and lies unconformably on the Gombe Formation. The maximum thickness of this formation is about 200 m (Carter et al., 1963; Arabi et al., 2009). While Zaborski (1998) suggested a thickness of 300 m for the Kerri-Kerri formation, Abubakar et al. (2010) suggested a thickness of about 320 m for the formation. The Gombe Formation is composed of sandstones, silt stones, and ironstones of Maastrichtian age. The Gombe Formation discharges water that infiltrates the Kerri-Kerri formation (Zaborski, 1998). The Pindiga Formation (240

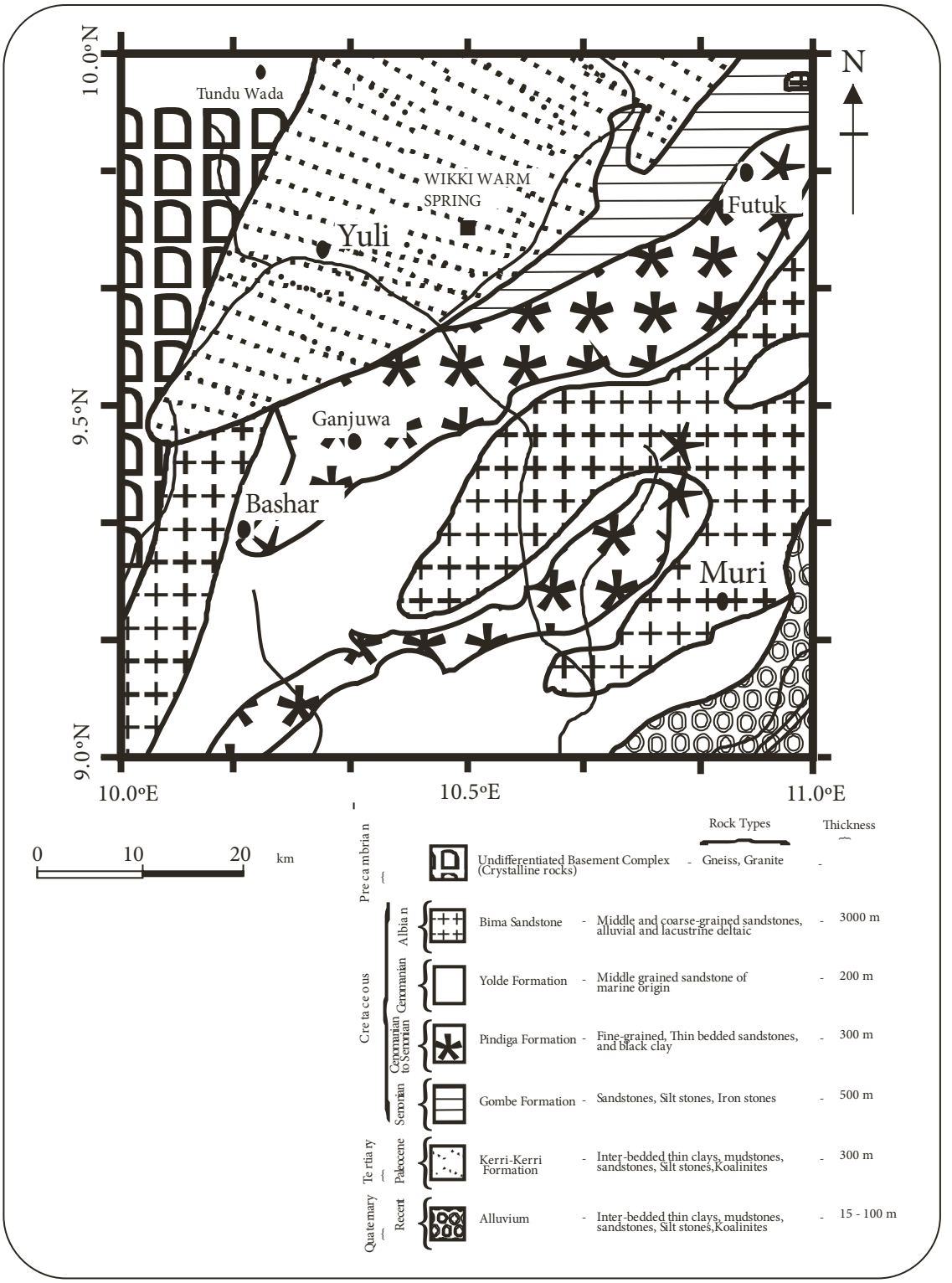

Figure 3. Geological map of the study area. The stratigraphy of our study area consists of the alluvium, the Kerri-Kerri Formation, the Gombe Sandstone Formation, the Pindiga Formation, the Yolde Formation, the Bima Formation, and basement rocks as the oldest.

m) consists mainly of shale mudstone with intercalations of limestone occurring in some areas (Abubakar et al., 2010). The Yolde Formation is believed to have a thickness of about 200 m and it is a transitional sequence between the continental Bima group and the marine deposits of the lower part of the Pindiga Formation. The Bima Formation is the oldest, most extensive, and thickest (about 3000 m; Zaborski, 1998) of the Cretaceous sedimentary formations in northeastern Nigeria (Arabi et al., 2009).

2. Materials and methods

2.1. Aeromagnetic data

Aeromagnetic data covering the study area collected in 1974 were obtained from the Geological Survey of Nigeria. The various map sheets obtained (sheets 171, 172, 192, and 193 having flight line spacing of 2 km and a nominal flight altitude of 152.4 m with NE–SW tie lines) were processed and merged together into a common dataset. The maps were scaled at 1:100,000 and, when put together, extended from 9°N to 10°N and from 10°E to 11°E. The maps were digitized on a selected grid of 1 km and contoured at 10 nT intervals. The International Geomagnetic Reference Field (IGRF 1975) was removed from the data. Figure 4 shows the total field aeromagnetic anomaly map of the study area. The analysis of magnetic anomalies used reduced-to-the-pole (RTP) data. The RTP correction applied assumed a declination of –1° and an inclination of –5° for this region utilizing the method of Silva (1986). Low-pass filtering was then applied to remove the effects of topography and regional features.

The magnetic anomaly map and the geologic map of the study area shows a good correlation between exposed geologic units and magnetic signatures. Notable positive anomalies are observed at the Tundu Wada (NW) region, reaching values of 40–120 nT. This tends to correspond with the exposed undifferentiated basement complex of

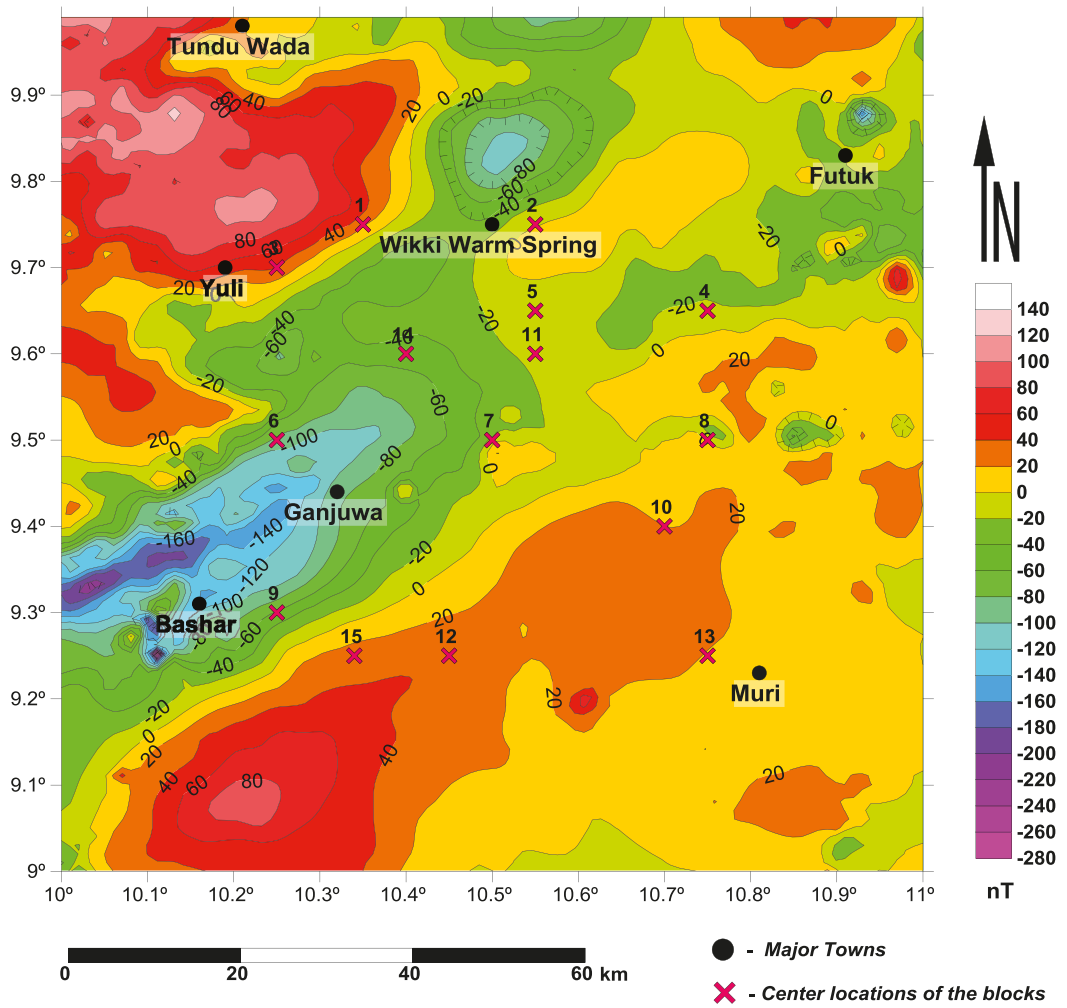

Figure 4. Total field magnetic anomaly map of the study area.

the geologic map. Negative anomalies have been noted in the north-central region of the map extending downwards to include Yuli, Ganjuwa, and Bashar towns and the WWS region. In general, negative anomalies were observed to follow a NE–SW trend in between Futuk and Bashar. We trace these anomalies to the Kerri-Kerri Formation extending well into the Bima sandstone–Yolde Formation around the town of Bashar. Positive anomalies ranging between 1 and 80 nT have also been noted at Muri and parts of the WWS region. The Bima sandstone–Yolde Formation, Marine Facies–Gombe sandstone, and parts of the Kerri-Kerri Formation towards the NE have been identified with these anomalies.

2.2. Centroid depth method for calculating DBMS

2.2.1. Random magnetization method

One of the methods for examining the thermal structure of the crust is the estimation of the CPD using aeromagnetic data (Smith et al., 1977; Okubo et al., 1985, 1989, 1994, 2003; Tsokas et al., 1998; Tanaka et al., 1999; Stampolidis and Tsokas, 2002; Dolmaz et al., 2005; Ates et al., 2005; Aydin et al., 2005; Qingqing et al., 2008; Li et al., 2010; Li, 2011; Bilim, 2011; Manea and Manea, 2011; Abd El Nabi, 2012; Hisarli et al., 2012; Saleh et al., 2013; Sayed et al., 2013; Abraham et al., 2014; Obande et al., 2014; Starostenko et al., 2014). Various studies have shown correlations between Curie temperature depths and average crustal temperatures, leading to viable conclusions regarding lithospheric thermal conditions in a number of regions around the world (Ross et al., 2006; Rajaram, 2007; Bouligand et al., 2009). Our calculation of DBMS is based on statistical methods of depth determination from the radial power spectrum of the magnetic field (Spector and Grant, 1970; Bhattacharyya and Leu, 1975, 1977; Okubo et al., 1985; Blakely, 1988; Tanaka et al., 1999; Ross et al., 2006; Trifonova et al., 2009; Bansal et al., 2011). These approaches assumed a random uniform uncorrelated distribution of sources. The power spectrum, P, for a 2D assemblage of bodies can be written as follow (Spector and Grant, 1970; Blakely, 1995).

$$P(k_x k_y) = 4\pi^2 C_m^2 |\Theta_m|^2 \left|\Theta_f\right|^2 e^{-2|k|z_t} \times \left(1 - e^{-|k|(z_b - z_t)}\right)^2 \quad (1)$$

Here, k_x and k_y are the wavenumbers in the x- and y-directions; C_m is a constant of proportionality; ϕ_m is the power spectrum of the magnetization; Θ_m and Θ_f are the directional factors related to the magnetization Θ_m and Θ_f geomagnetic field, respectively; and z_t and z_b are the top and bottom depths of the magnetic sources. After annual averaging, Eq. (1) can be written as

$$P(|k|) = A_1 e^{-2|k|z_t}\left(1 - e^{-|k|(z_b - z_t)}\right)^2 \quad (2)$$

where A_1 is a constant. Eq. (2) can be simplified to compute the centroid depth z_o of the magnetic source (Spector and Grant, 1970; Bhattacharyya and Leu, 1975, 1977; Okubo et al., 1985) from the low-wavenumber part of the power spectrum as follows.

$$\ln\left(\frac{P(|k|)^{1/2}}{|k|}\right) = \ln A_2 - |k|z_o \quad (3)$$

Here, ln is the natural logarithm and A_2 is a constant. Eq. (2) is also simplified to compute the top of magnetic sources z_t by assuming that the signals from the source tops dominate the spectrum. For wavelengths less than about twice the thickness of the layer (Tanaka et al., 1999), Eq. (2) approximately becomes:

$$\ln\left[P(|k|)^{1/2}\right] = \ln A_3 - |k|z_t \quad (4)$$

The estimate of DBMS is performed in two steps: the first is to calculate the z_o of the deepest magnetic sources using Eq. (3) and the second is to calculate z_t of the deepest magnetic sources using Eq. (4). This approach is known as the centroid depth method (Bansal et al., 2011). Bhattacharyya and Leu (1975) derived the equations for calculating the centroid and top depths for 2D structures with arbitrary polygon cross-sections, and Okubo et al. (1985) suggested that the same equations are applicable to any 3D shaped bodies. The DBMS can be calculated as follows.

$$z_b = 2z_o - z_t \quad (5)$$

2.2.2. Fractal magnetization method

This approach assumes that the observed power spectrum is equivalent to the random magnetization model multiplied by the effect of fractal magnetization (Salem et al., 2014). The fractal source distribution method provides better estimates than the assumption of an uncorrelated source distribution (Bansal et al., 2011). Real geologic situations are often multilayered. The application of Eq. (3) results in larger centroid depth values, even if small block sizes are used (Bansal et al., 2011; Li et al., 2013). Eqs. (3) and (4) assume a random and uncorrelated distribution of sources, whereas in reality the source distribution follows a fractal/scaling distribution (Pilkington and Todoeschuck, 1990, 2004; Maus and Dimri, 1995; Bansal et al., 2010, 2011). Methods that account for this distribution have been developed for calculating depths from 2D field data (Pilkington and Todoeschuck, 1993, 2004; Pilkington et al., 1994; Maus and Dimri, 1995, 1996; Dimri, 2000; Dimri et al., 2003; Bansal et al., 2011). For a fractal distribution of sources, the radial average power spectrum of the magnetization $\phi_m(k)$ follows the relation

$$\phi_m(k) \propto k^{-\beta} \quad (6)$$

where β is the fractal/scaling exponent. Its value depends on the lithology and heterogeneity of the subsurface (Bansal et al., 2010, 2011; Salem et al., 2014).

We propose to estimate the DBMS using a similar two-step approach for the centroid method but with the fractal method (Bansal et al., 2011). For a fractal distribution of sources, the power spectrum of Eq. (3) for computing the centroid depth can be rewritten after combining Eqs. (3) and (6).

$$\ln\left(k^{\beta} \times \frac{P(k)}{k^2}\right) = A_4 - 2kz_o \quad (7)$$

The top depth to the deepest magnetic sources can be estimated from the fractal approach by combining Eqs. (4) and (6).

$$\ln\left(k^{\beta} \times P(k)\right) = A_5 - 2kz_t \quad (8)$$

Bouligand et al. (2009) summarized published estimates for the fractal parameter β within various contexts and from aeromagnetic studies in the continental domain and noted a value of 1.5 for sedimentary (sandstone) lithology from Maus and Dimri (1995). Therefore, we fix β = 1.5 for 2D bodies in our study area since it is a sedimentary (sandstone) terrain. In the fractal case, prefiltering as suggested by Okubo et al. (1985) becomes redundant (Bansal et al., 2011). Nevertheless, we applied the appropriate filtering to the data before computing the DBMS. For the adopted method, only a scaling exponent of less than 2 will work; otherwise, $P(k)/k^2$ would be overcorrected (Bansal et al., 2011). The DBMS is then calculated from Eq. (5).

2.3. Application to magnetic dataset

In the estimation of depths to the Curie temperature in Oregon, for example, Connard et al. (1983) divided a magnetic survey into overlapping cells (77 × 77 km^2) and calculated a radially averaged power spectrum for each cell. However, the spectrum of the map only contains depth information to a depth of length/2π (Shuey et al., 1977). If the source bodies have bases deeper than L/2π, the spectral peak occurs at a frequency lower than the fundamental frequency for the map and cannot be resolved by spectral analysis (Salem et al., 2000). We first apply the spectral method to the main grid of our study area (110 × 110 km^2) to determine the DBMS for the grid to be used for comparison. However, since it is the center of windows or blocks chosen that is analyzed for the DBMS, the dimensions of the main grid will provide depth information for the center of the block, which is farther away from the principal focus of this study (the WWS region). In light of this explanation and given the geology of the region, we adopted the suggestion of Okubo et al. (1985) on the minimal block size to use. The methods of Spector and Grant (1970) and Okubo et al. (1985), which examined the spectral knowledge included in subregions of magnetic data, are used for our analysis. This algorithm (and all other magnetic methods) only computes depths to the bottoms of magnetization contrasts. Whether or not these depths represent Curie point transitions is an interpretation that must be supported by other independent evidence (Okubo et al. 1985; Trifonova et al. 2009). Li et al. (2010) compared results of z_b from a fixed window size of 99.2 × 99.2 km^2 and reduced window size of 68.2 × 68.2 km^2 and showed that the map of z_b estimated using a smaller window has a higher resolution and that the general pattern with important features of z_b have little changes, with only minor local variations. They further went on to test a window of 144.15 × 144.15 km^2 and submitted that, again, the general pattern and important features were kept almost the same despite being at a much lower resolution. They concluded that there are no large or persistent patterns caused by changing windows. We adopted the size of an individual map (55 × 55 km^2) of the four-map consortium used for this study to represent our block size. The choice of 55 × 55 km^2 block dimension slide across the magnetic anomaly map (Figure 5) was necessary because of the complexity of the geology of the area and the need to sample more data points while preserving the spectral peak, as suggested by Okubo et al. (1985). In addition to the initial six blocks realized (at 50% overlap), we obtain at random nine additional blocks guided by the concentration of prominent magnetic anomalies on the map. To alleviate the problem of contamination, Ross et al. (2006) placed center points for subregions within geologic provinces to capture and emphasize aeromagnetic anomalies associated with each province. They added that the method was in contrast to previous methods that used uniform grids of overlapping subregions, forcing center points to follow a secondary uniform grid. Trifonova et al. (2009) selected additional windows over geophysically homogeneous regions to add 5 more blocks (each of them comprising a single prominent magnetic anomaly) to their processing grid. Bouligand et al. (2009) mapped model parameters for their study by estimating their values within a sliding window swept over the study area. We felt the need to sample more points within the WWS location and this method realized that objective. Selecting windows over geologically/geophysically homogeneous regions rather than margins of provinces is another consideration that is very useful in the process of choosing window sizes to ascertain that one is not missing the spectral peaks (Ross et al., 2006; Ravat et al., 2007). Determination of the size of blocks to be

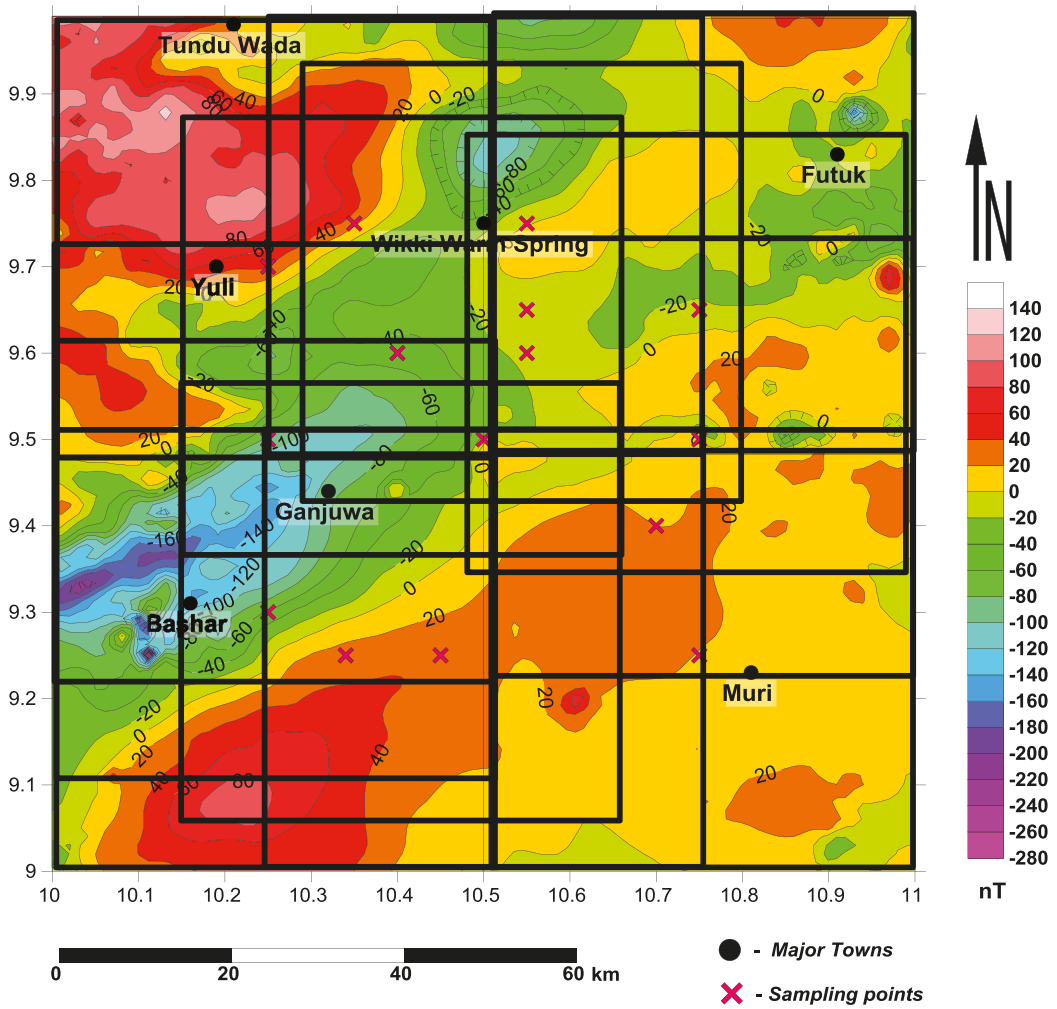

Figure 5. Total field magnetic anomaly map of the study area illustrating section of overlapping blocks. The coordinates at the center of each block represent the assigned location of the reulting depth estimation.

used for calculations requires a compromise between the spatial resolution and preservation of the long-wavelength part of the spectrum. Even if the technique provides an accurate z_b there is no guarantee that z_b represents the Curie temperature depth. A variety of geologic reasons exist for truncated magnetic sources that are unrelated to crustal temperatures (Trifonova et al., 2009). All depth estimates must be carefully performed and assessed using tectonic framework, geological and shallow as well as deep geophysical evidence, and heat flow modeling (Ravat et al., 2007). Figure 4 shows an illustration of the selection of overlapping blocks. Fast Fourier transform was used to convert the space domain grid data to the Fourier domain. The log of the radially averaged power spectrum for fractal distribution of sources of each block was computed using Eqs. (7) and (8). The depth values were then computed from Eq. (5). Tanaka et al. (1999) suggest computing z_t from the high-wavenumber part of the spectrum. Calculating the depth to the top of magnetic layer from the higher wavenumber portion may be appropriate for identifying the depth to the shallowest magnetic material, if one is mapping a single layer representing the bulk of the magnetization (Spector and Grant, 1970; Bansal et al., 2011; Salem et al., 2014). Nevertheless, to compute the DBMS, the depth to the top of the deepest layer is required (Bansal et al., 2011). Therefore, we use the straight slope part of the spectrum next to the peak (from wavenumbers higher than the peak) to estimate the depth to the top of the single layer or the deepest magnetic layer in multilayer situations (Bansal et al., 2011, 2013; Bansal and Anand, 2012, Salem et al., 2014). This is important because multilayer magnetization situations are common, especially in continental areas, and in those cases, to determine the magnetic bottom, one needs to select the slope related to the deepest magnetic layer (Salem et al., 2014). For the 55 × 55 km^2 window, we encounter the

multilayer situation in the analysis of windows 1, 6, 7, 8, 12, 13, 14, and 15 and also found spectral peaks for nine of the blocks selected (blocks 2, 4, 5, 6, 8, 11, 12, 14, and 15), representing more than 60% of the blocks considered for this study (Figure 6). While large windows could preferentially capture more contributions from deeper local bottoms of magnetic sources, they could also smear local features that potentially have deeper bottoms, and,

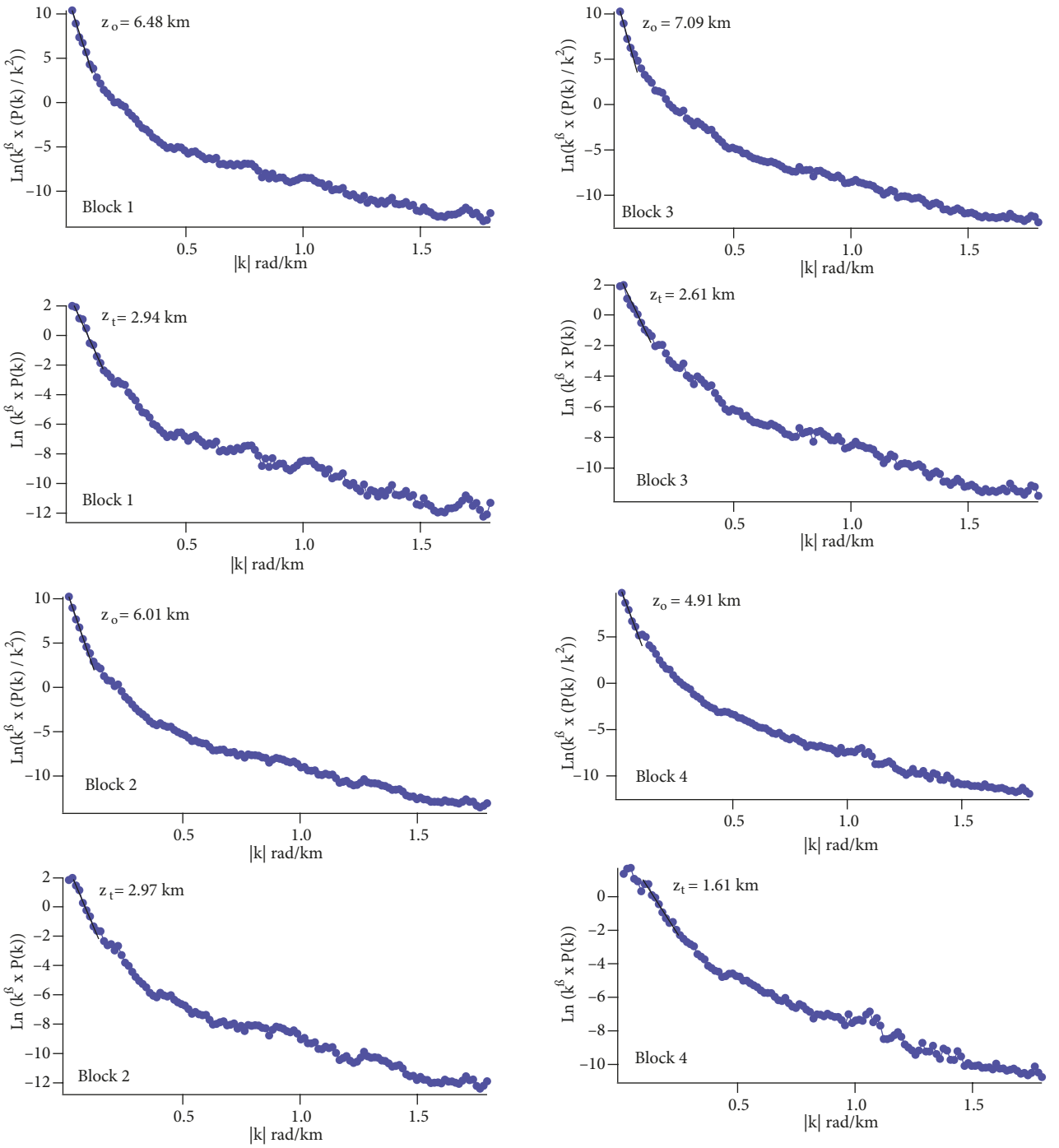

Figure 6. Examples of radially averaged power spectra for estimation of DBMS using the fractal distribution of sources method on 55 × 55 km blocks. Blocks/windows 2, 4, 5, 6, 11, and 15 show notable peaks as seen on the z_t power spectrum. A multilayer situation is seen in the analysis of windows 1, 6, 7, 8, 12, 13, 14, and 15.

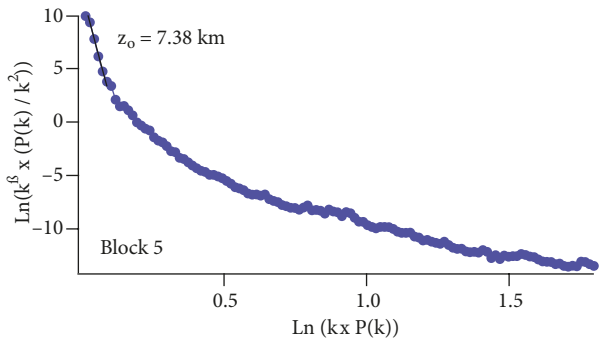

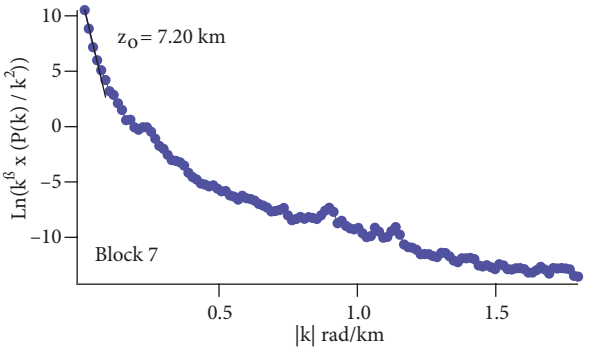

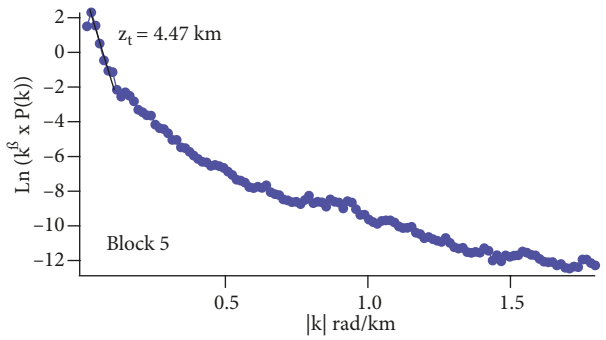

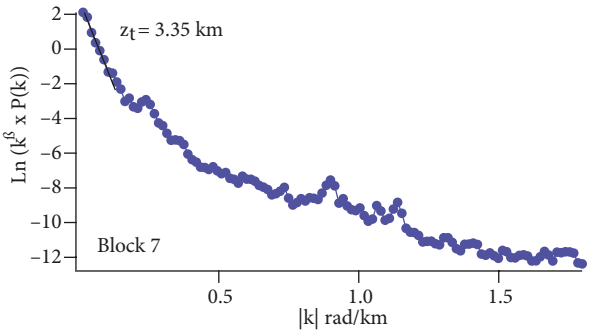

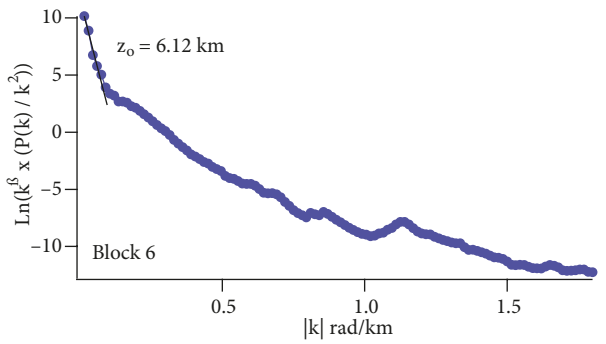

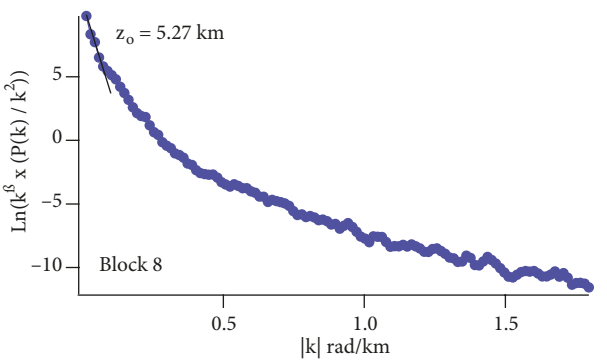

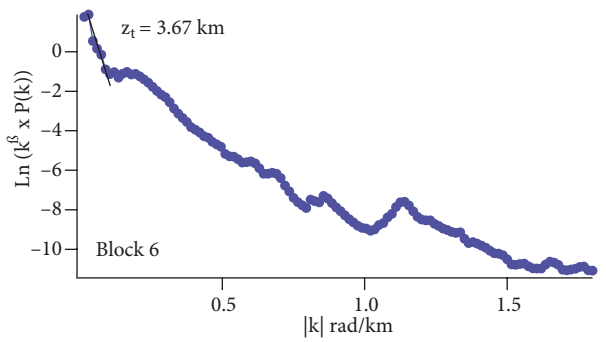

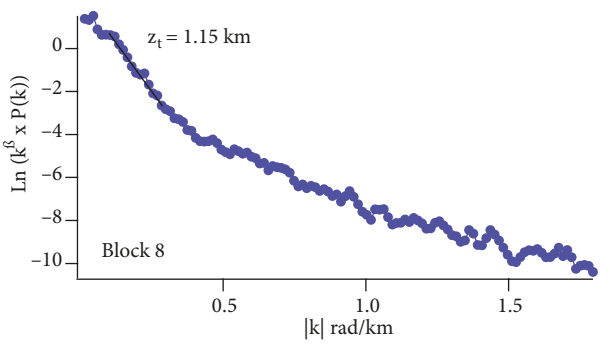

Figure 6. (Continued.)

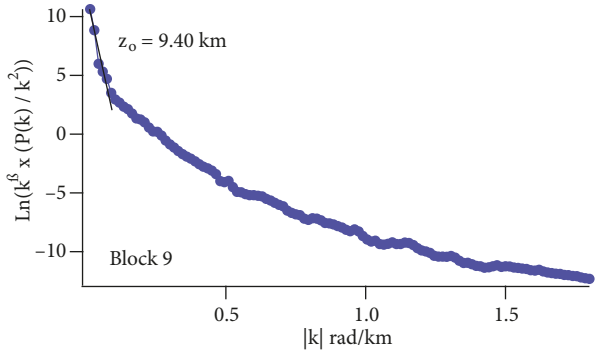

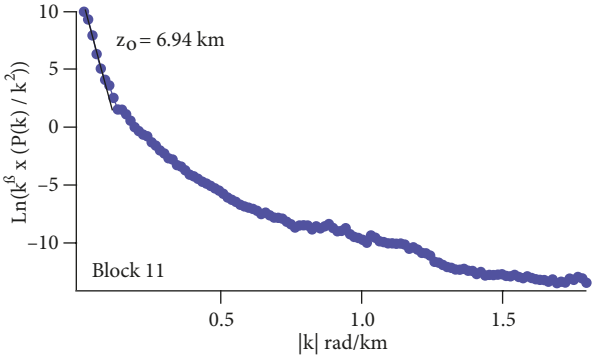

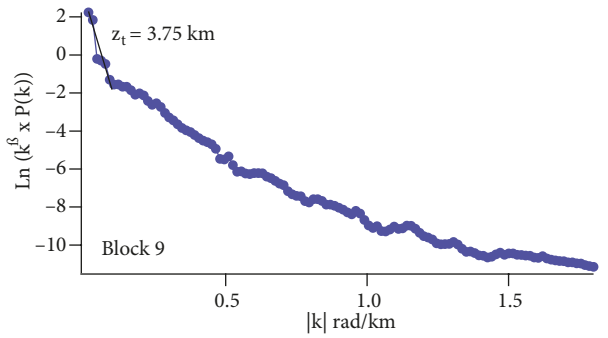

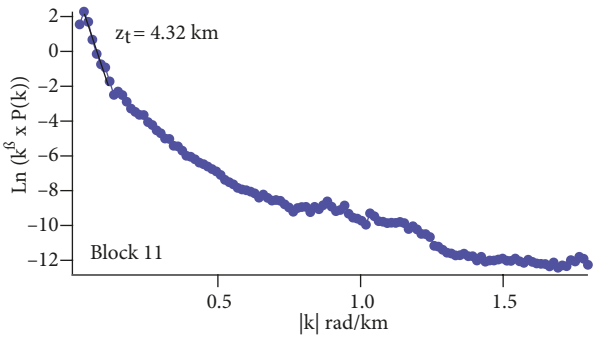

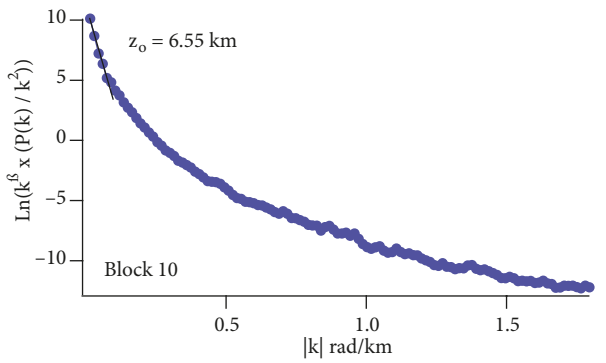

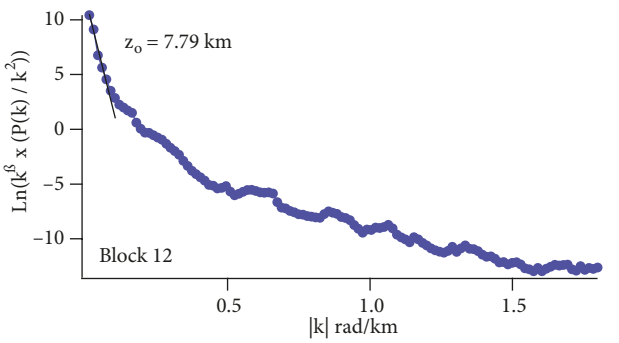

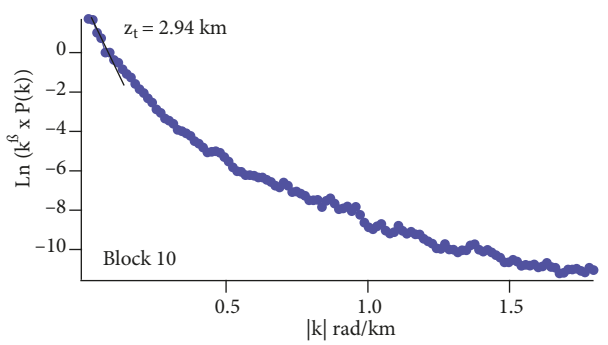

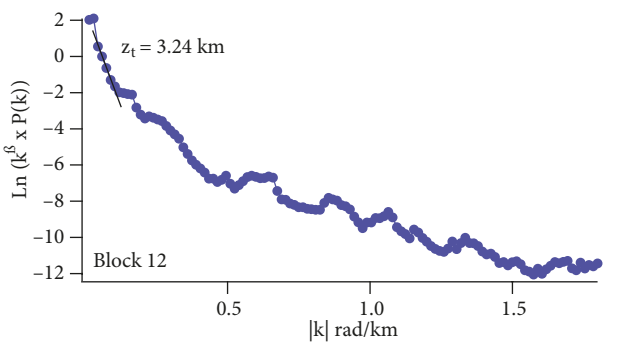

Figure 6. (Continued.)

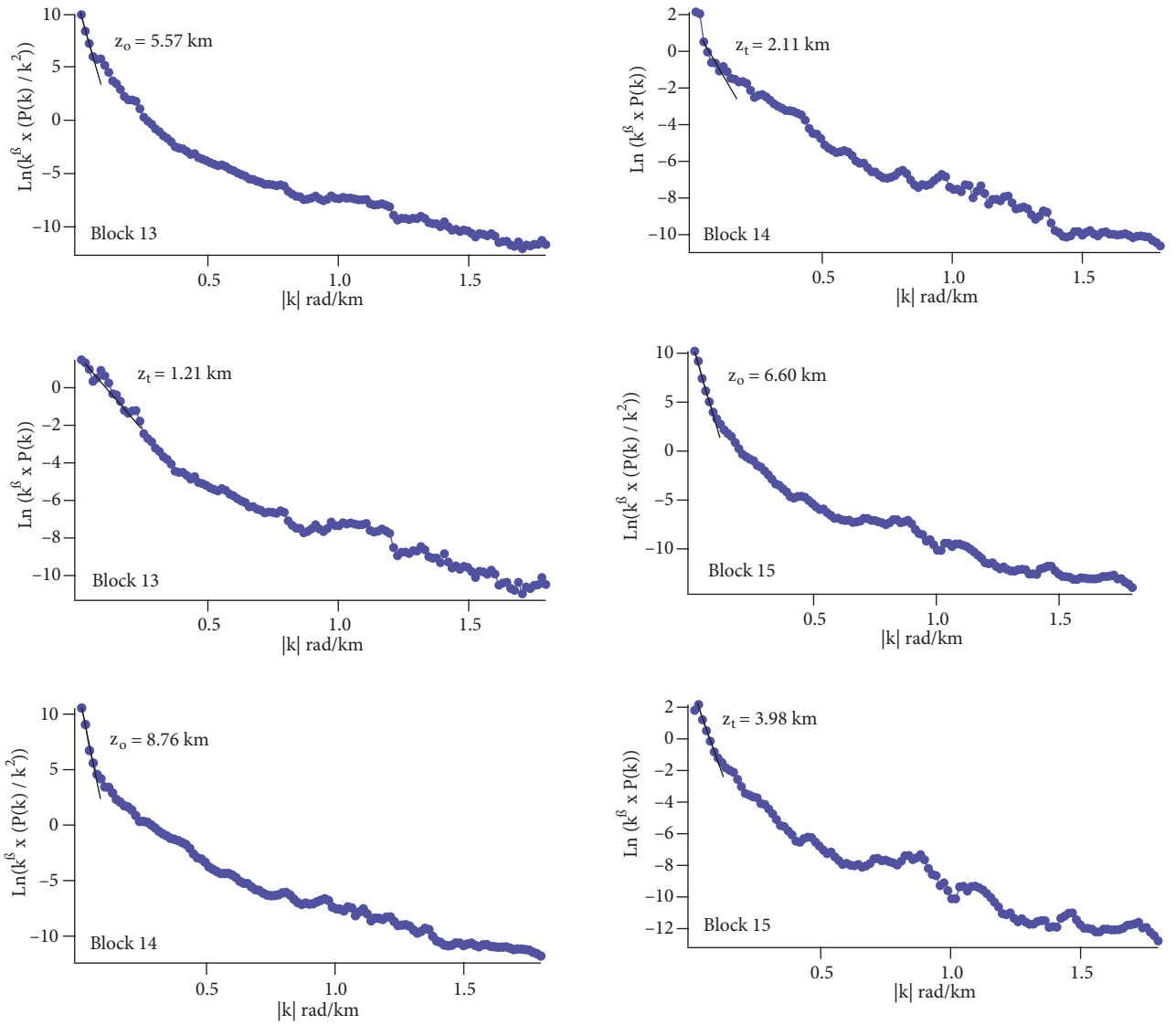

Figure 6. (Continued.)

by enlarging the window, long wavenumber components and/or spectra of uniformly magnetized layer could also gain more portions of power, enough to disguise the peak on the amplitude spectrum (Li et al., 2010). The shape of the radial power spectrum as calculated in previous studies ideally should display a peak at low wavenumbers. However, the absence of a peak at low wavenumbers may indicate fractal behavior of the magnetization (Bouligand et al., 2009). Larger wavenumbers were not considered because they are likely from noises and they are not needed, according to numerical and theoretical tests (Li et al., 2013). Figure 7 shows the power spectrum calculation plot for the main grid (110 × 110 km^2).

The Table shows estimated DBMS results from fractal sources. We evaluate the standard and statistical errors of the power density spectrum from the linear fit using the definition of error adopted by Trifonova et al. (2009).

2.4. Conductive heat flow

The basic relation for conductive heat transport is Fourier's law. Tanaka et al. (1999) showed that any given depth to a thermal isotherm is inversely proportional to heat flow. In a one-dimensional case under assumptions that the direction of the temperature variation is vertical and the temperature gradient dT/dz is constant, Fourier's law takes the following form:

$$q = k\frac{dT}{dz} \tag{12}$$

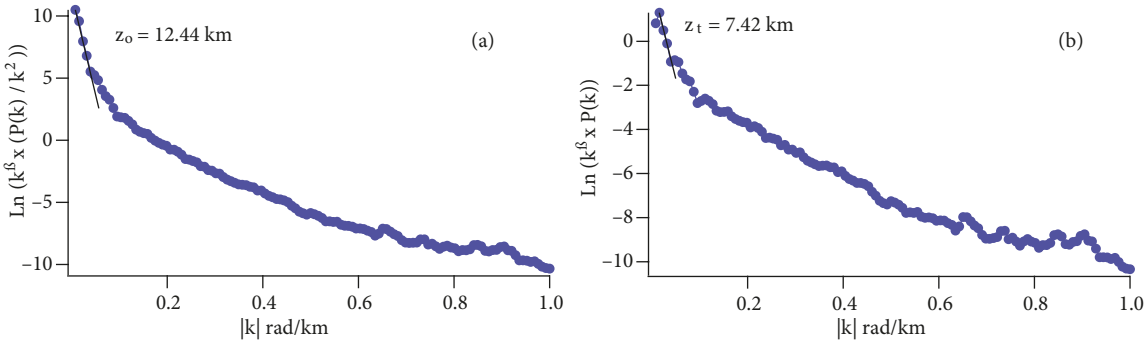

Figure 7. Examples of radially averaged power spectrum for estimation of DBMS using the fractal distribution of sources method from the two-dimensional magnetic anomaly data of the main grid (110 × 110 km). **(a)** shows a value of 12.44 km as the centroid depth and **(b)** shows an estimation of depth to the top as 7.42 km, both obtained using the gradient of spectra defined as $\ln\left(k^{\beta}\times\frac{P(k)}{k^2}\right)$ and $\ln\left(k^{\beta}\times P(k)\right)$,, where |k| is the wavenumber and P(k) is the radially average power spectrum.

where q is the heat flux and k is the coefficient of thermal conductivity.

According to Tanaka et al. (1999), the Curie temperature (θ) can be obtained from the CPD z_b and the thermal gradient dT/dz using the following equation:

$$\theta = \left(\frac{dT}{dz}\right) z_b \tag{13}$$

In this equation, it is assumed that the surface temperature is zero and is dT/dz constant.

This relation implies that regions of high heat flow are associated with shallower isotherms, whereas regions of lower heat flow are associated with deeper isotherms (Ross et al., 2006). An average surface heat flow value was computed using heat flow equations (Tanaka et al., 1999) and was based on possible Curie point temperature of 580 °C using a thermal conductivity of 2.5 $Wm^{-1}\,°C^{-1}$, given by Stacey (1977) as the average for igneous rocks.

3. Discussion and conclusions

The estimated DBMS results from 55 × 55 km^2 windows show a minimum depth of 8.21 ± 1.06 km, whereas a maximum depth of 15.41 ± 1.89 km (Table) was estimated

Table. Estimated depth to the bottom of magnetic sources (DBMS) from fractal distribution of sources and calculated heat flow values with their uncertainties for each of the blocks.

Block	Coordinates (degrees)		Depth to centroid (z_o) (km)	Depth to top (z_t) (km)	Depth to bottom, DBMS (z_b) (km)
	Longitude	Latitude			
1	10.35	9.75	6.48 ± 0.06	2.94 ± 0.01	10.00 ± 0.23
2	10.55	9.75	6.00 ± 0.05	2.97 ± 0.04	9.05 ± 0.28
3	10.25	9.70	7.08 ± 0.34	2.62 ± 0.10	11.56 ± 1.53
4	10.75	9.65	4.91 ± 0.04	1.61 ± 0.18	8.21 ± 1.06
5	10.55	9.65	7.38 ± 0.31	4.47 ± 0.21	10.30 ± 1.34
6	10.25	9.50	6.61 ± 0.10	3.67 ± 0.16	9.55 ± 0.70
7	10.50	9.50	7.20 ± 0.09	3.35 ± 0.06	11.06 ± 0.45
8	10.75	9.50	5.27 ± 0.08	1.15 ± 0.06	9.39 ± 0.78
9	10.25	9.30	9.39 ± 0.34	3.75 ± 0.17	15.04 ± 1.78
10	10.70	9.40	6.55 ± 0.06	2.94 ± 0.31	10.17 ± 1.24
11	10.55	9.60	6.94 ± 0.27	4.32 ± 0.16	9.55 ± 1.12
12	10.45	9.25	7.79 ± 0.04	3.24 ± 0.21	12.35 ± 0.96
13	10.75	9.25	5.57 ± 0.08	1.21 ± 0.02	9.92 ± 0.45
14	10.40	9.60	8.76 ± 0.34	2.11 ± 0.09	15.41 ± 1.89
15	10.34	9.25	6.60 ± 0.09	3.98 ± 0.20	9.22 ± 0.72

for the study area, representing an average value of 10.72 ± 0.54 km. The shallowest DBMS, ranging between 8 and 10 km, is obtained northeastwards of the area covered by this study (towards Futuk) and at the Muri (southeastern) regions of the map (Figure 8). These regions are farther from the WWS region and are located below the Marine Facies Pindiga Formation–Gombe sandstone and the Bima sandstone formation. A concentration of major geologic lineaments (faults and fractures) is noticed in these regions, leading to the conclusion that the shallow DBMS obtained could be due to magmatic intrusions at depth. Kurowska and Schoeneich (2010) suggested that the heating effect of volcanic and intrusive activity on cretaceous sedimentary basins, especially the Benue Trough, as well as the basement complex contributed to the development of local thermal anomalies observed in the region. The sources of seismicity in Nigeria include inhomogeneities and zones of weakness in the crust from various episodes of magmatic intrusions and other tectonic activities (Eze et al., 2011). We propose that inadequate fluid interaction with the subsurface thermal structure at these locations is responsible for the lack of surface manifestations of geothermal signatures. Tanaka et al. (1999) pointed out that the CPDs are shallower than

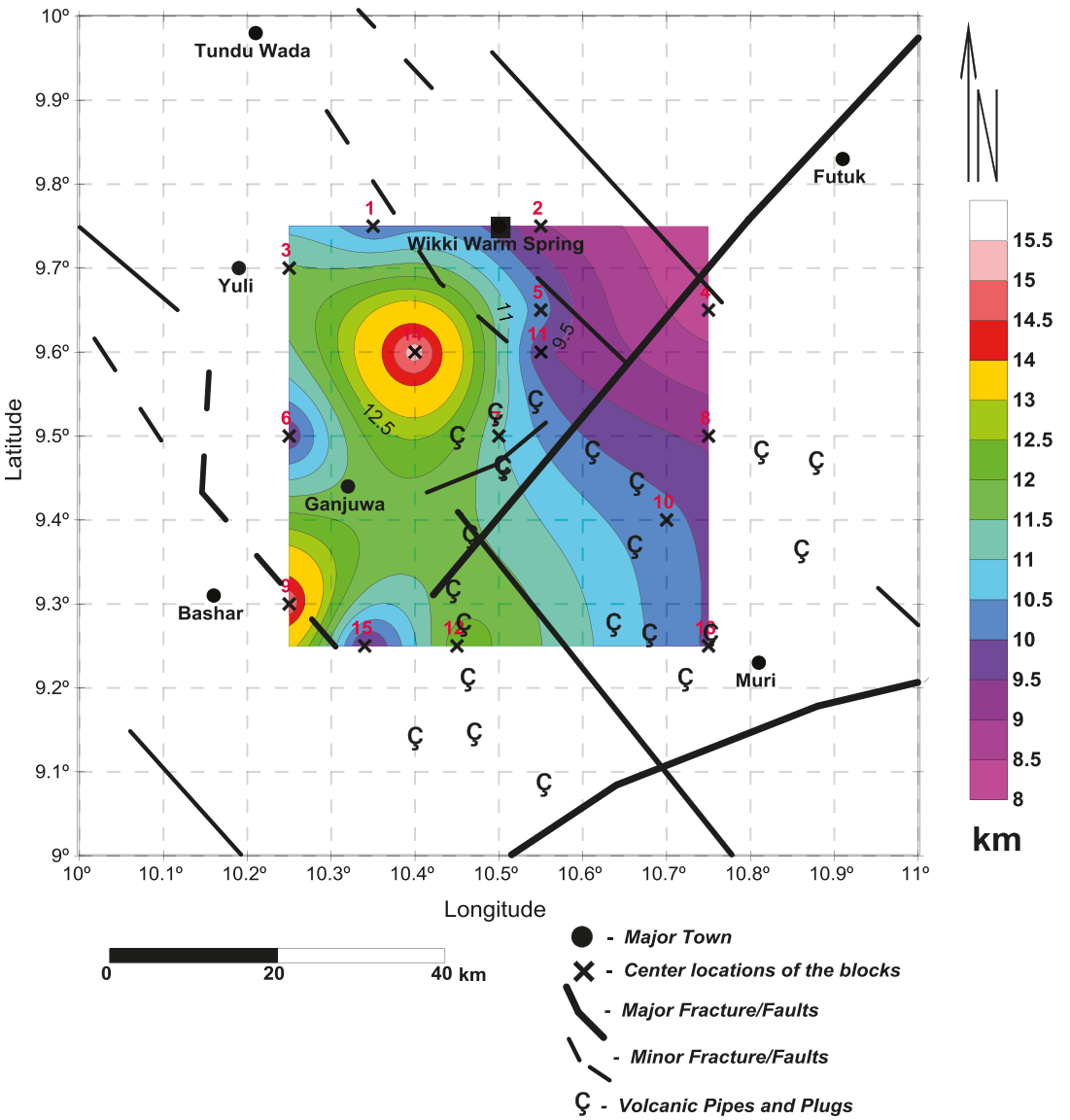

Figure 8. Map of DBMS for fractal distribution of sources in the study area. Depths were plotted using data from the Table. The lineaments in the West African Rift system of the study area are also shown on the map to reveal the hidden architecture of the rock basement.

about 10 km at volcanic and geothermal areas. At the WWS location, DBMS ranges between 9.5 and 10 km. This region lies on the Kerri-Kerri Formation of Tertiary age, which is composed of sandstone, silt stones, kaolinites, and grits, and underneath this lies the Gombe Formation (Ubaru, 2000). We propose that the heat source for the WWS could be connected with the shallow DBMS obtained in that part of the Gombe sandstone formation lying underneath the Kerri-Kerri Formation and it could be influenced by adjoining contacts. The effect of magmatic intrusions in the formation could have provided the heat contacts of which favorable geologic feature (faults) and fluid brought the geothermal signatures to the surface in the Kerri-Kerri Formation. Cratchley et al. (1984) suggested the presence of warm springs and hot brines along the axis of the Benue Trough, with abnormally hot material beneath the trough at comparatively shallow depths. The northwestern (around Yuli) and southwestern (around Bashar) areas show deeper DBMS ranges, between 12 and 15 km, and are traced to the Bima Formation with parts of the Gombe Formation towards the south. Our depth results do not agree with those of Eletta and Udensi (2012), whose study area cuts across half of our study area to the south. Their Curie depths of 2–8.4 km depicts underestimation given the method adopted of random distribution of sources. We observed that no mention was made on data processing before implementation of spectral analysis techniques. For example, reduction to pole, which is a classical procedure for their adopted method, was not performed, and application of appropriate filtering was not stated; this could have affected their results. Our computed average z_t gave a value of 2.95 km for the study area.

The method used for DBMS calculation is very subjective and has to be constrained with independent information for a region. Because DBMS values are estimated from magnetic data, they may represent temperatures of petrological/compositional boundaries (Bansal et al., 2013). Information about temperature measurements in depth or data about expected mineralogy in the region are useful in this regard. However, we have been constrained by lack of data on temperature measurement at depths in the region of study. Nevertheless, we compare our result with that of Kurowska and Schoeneich (2010), which is closer to our study region. Their geothermal gradient map shows a higher value (58.4 °C/km) towards our study area, which reinforces our confidence in the computed geothermal gradient of 59.18 °C/km for the WWS source location and an average of 54.11 °C/km for the entire study area. For places where heat flow information is inadequate, the depth to the Curie temperature isotherm may provide a proxy for temperature-at-depth (Ross et al., 2006). Our average geothermal gradient implies an average heat flow value of 135.27 ± 3.16 mW/m^2. Heat flow in excess of about 80–100 mW/m^2 indicates anomalous geothermal conditions in the subsurface (Sharma, 2004). In spite of limitations, DBMS/Curie depths can be used to complement geothermal data in regions where deep boreholes are unavailable (Bansal et al., 2011). The presence of the WWS in the study area and the estimated average heat flow obtained indicates anomalous condition in the subsurface.

Obande et al.'s (2014) average DBMS of 8 km from uncorrelated distribution of magnetic sources appears close to our average value of 10.72 ± 0.54 km from fractal sources. However, it is expected that proper application of Eq. (3) results in larger centroid depth values, even if small window/block sizes are used (Bansal et al., 2011), and without corrections for fractal exponents, the inversion scheme is not sensitive to Curie depth variations and will give overestimations (Li et al., 2013). Although proper implementation of Obande et al.'s (2014) method would seem adequate for the analysis, we respectfully disagree with their results as regards depths to the centroid (z_o) of the magnetic source. Their application of the methodology in estimating z_o (and therefore CPD) is not theoretically based. They estimated depth to the centroid by fitting a straight line directly to the same spectrum, resulting in lower depth estimates. Both z_t and z_o of magnetic sources were evaluated from the same power spectrum instead of adherence to established theoretical guidelines as proposed by Tanaka et al. (1999) and explained earlier in this manuscript. The introduction of fractal exponents in the inversion effectively suppresses lateral correlations of magnetic sources (Pilkington and Todoeschuck, 1993, 1995; Maus et al., 1997; Ravat et al., 2007; Bouligand et al., 2009) and leads to z_b conformable to known geological constraints (Li et al., 2013).

Results of DBMS from the 110 × 110 km^2 windows show a value of 17. 46 km (Figure 7) with estimated geothermal gradient of 33.22 °C/km. This result is obtained for the center of the main grid (which appears farther from the WWS source location). However, we observed that the thermal gradient computed from this depth is closer to the lower bound range of values obtained from the 55 × 55 km^2 block sizes (37.63 to 70.66 °C/km). The generally shallow DBMS values obtained in the study area and the attendant high heat flow values emphasizes the effects of large-scale tectonic events, particularly the basin-initiating event, as a major influence on thermal history. Blackwell and Steele (1988) showed that the scale of effect of control of temperature on sedimentary basins is larger for internal thermal events (intrusion or diapirism). Potential regions for geothermal exploration are characterized by high heat flow, high temperature gradient, and therefore shallow DBMS (Bansal et al., 2011). Kuroska and Schoeneich (2010) implied that the water of the warm spring was heated by a geothermal gradient on its way from unknown depths,

about 10 km at volcanic and geothermal areas. At the WWS location, DBMS ranges between 9.5 and 10 km. This region lies on the Kerri-Kerri Formation of Tertiary age, which is composed of sandstone, silt stones, kaolinites, and grits, and underneath this lies the Gombe Formation (Ubaru, 2000). We propose that the heat source for the WWS could be connected with the shallow DBMS obtained in that part of the Gombe sandstone formation lying underneath the Kerri-Kerri Formation and it could be influenced by adjoining contacts. The effect of magmatic intrusions in the formation could have provided the heat contacts of which favorable geologic feature (faults) and fluid brought the geothermal signatures to the surface in the Kerri-Kerri Formation. Cratchley et al. (1984) suggested the presence of warm springs and hot brines along the axis of the Benue Trough, with abnormally hot material beneath the trough at comparatively shallow depths. The northwestern (around Yuli) and southwestern (around Bashar) areas show deeper DBMS ranges, between 12 and 15 km, and are traced to the Bima Formation with parts of the Gombe Formation towards the south. Our depth results do not agree with those of Eletta and Udensi (2012), whose study area cuts across half of our study area to the south. Their Curie depths of 2–8.4 km depicts underestimation given the method adopted of random distribution of sources. We observed that no mention was made on data processing before implementation of spectral analysis techniques. For example, reduction to pole, which is a classical procedure for their adopted method, was not performed, and application of appropriate filtering was not stated; this could have affected their results. Our computed average z_t gave a value of 2.95 km for the study area.

The method used for DBMS calculation is very subjective and has to be constrained with independent information for a region. Because DBMS values are estimated from magnetic data, they may represent temperatures of petrological/compositional boundaries (Bansal et al., 2013). Information about temperature measurements in depth or data about expected mineralogy in the region are useful in this regard. However, we have been constrained by lack of data on temperature measurement at depths in the region of study. Nevertheless, we compare our result with that of Kurowska and Schoeneich (2010), which is closer to our study region. Their geothermal gradient map shows a higher value (58.4 °C/km) towards our study area, which reinforces our confidence in the computed geothermal gradient of 59.18 °C/km for the WWS source location and an average of 54.11 °C/km for the entire study area. For places where heat flow information is inadequate, the depth to the Curie temperature isotherm may provide a proxy for temperature-at-depth (Ross et al., 2006). Our average geothermal gradient implies an average heat flow value of 135.27 ± 3.16 mW/m^2. Heat flow in excess of about 80–100 mW/m^2 indicates anomalous geothermal conditions in the subsurface (Sharma, 2004). In spite of limitations, DBMS/Curie depths can be used to complement geothermal data in regions where deep boreholes are unavailable (Bansal et al., 2011). The presence of the WWS in the study area and the estimated average heat flow obtained indicates anomalous condition in the subsurface.

Obande et al.'s (2014) average DBMS of 8 km from uncorrelated distribution of magnetic sources appears close to our average value of 10.72 ± 0.54 km from fractal sources. However, it is expected that proper application of Eq. (3) results in larger centroid depth values, even if small window/block sizes are used (Bansal et al., 2011), and without corrections for fractal exponents, the inversion scheme is not sensitive to Curie depth variations and will give overestimations (Li et al., 2013). Although proper implementation of Obande et al.'s (2014) method would seem adequate for the analysis, we respectfully disagree with their results as regards depths to the centroid (z_o) of the magnetic source. Their application of the methodology in estimating z_o (and therefore CPD) is not theoretically based. They estimated depth to the centroid by fitting a straight line directly to the same spectrum, resulting in lower depth estimates. Both z_t and z_o of magnetic sources were evaluated from the same power spectrum instead of adherence to established theoretical guidelines as proposed by Tanaka et al. (1999) and explained earlier in this manuscript. The introduction of fractal exponents in the inversion effectively suppresses lateral correlations of magnetic sources (Pilkington and Todoeschuck, 1993, 1995; Maus et al., 1997; Ravat et al., 2007; Bouligand et al., 2009) and leads to z_b conformable to known geological constraints (Li et al., 2013).

Results of DBMS from the 110 × 110 km^2 windows show a value of 17. 46 km (Figure 7) with estimated geothermal gradient of 33.22 °C/km. This result is obtained for the center of the main grid (which appears farther from the WWS source location). However, we observed that the thermal gradient computed from this depth is closer to the lower bound range of values obtained from the 55 × 55 km^2 block sizes (37.63 to 70.66 °C/km). The generally shallow DBMS values obtained in the study area and the attendant high heat flow values emphasizes the effects of large-scale tectonic events, particularly the basin-initiating event, as a major influence on thermal history. Blackwell and Steele (1988) showed that the scale of effect of control of temperature on sedimentary basins is larger for internal thermal events (intrusion or diapirism). Potential regions for geothermal exploration are characterized by high heat flow, high temperature gradient, and therefore shallow DBMS (Bansal et al., 2011). Kuroska and Schoeneich (2010) implied that the water of the warm spring was heated by a geothermal gradient on its way from unknown depths,

in an unconfined sandstone aquifer. We hope that this study has provided the much needed depth information to further geothermal exploration activity in the region.

We conclude that the low DBMS obtained at the WWS region could be due to intrusions or diapirism in the subsurface. The volcanic pipes spotted in the region, geologic lineaments, faults, and multiple fractures in the rock units strengthen this conclusion. We therefore recommend detailed temperature measurement at various depths through a series of boreholes to be located at adequate intervals within the WWS location to provide the much needed data for further exploration and exploitation of the geothermal energy resource potentials of the WWS region.

Acknowledgments
We are grateful to all the anonymous reviewers and editors whose thorough, critical, and constructive comments contributed to improve this manuscript.

References

Abd-El-Nabi SH (2012). Curie point depth beneath the Barramiya-Red Sea coast area estimated from aeromagnetic spectral analysis. J Asian Earth Sci 43: 254–266.

Abraham EM, Lawal KM, Ekwe AC, Alile O, Murana KA, Lawal AA (2014). Spectral analysis of aeromagnetic data for geothermal energy investigation of Ikogosi Warm Spring - Ekiti State, southwestern Nigeria. Geothermal Energy 2: 1–21.

Abubakar YI, Umego MN, Ojo SB (2010). Evolution of Gongola basin upper Benue Trough northeastern Nigeria. Asian J Earth Sci 3: 62–72.

Ajayi CO, Ajakaiye DE (1981). The origin and peculiarities of the Nigerian Benue Trough: another look from recent gravity data obtained from the middle Benue. Tectonophysics 80: 285–303.

Alagbe OA, Sunmonu LA (2014). Interpretation of aeromagnetic data from Upper Benue Basin, Nigeria using automated techniques. IOSR Journal of Applied Geology and Geophysics 2: 22–40.

Arabi AS, Nur A, Dewu BBM (2009). Hydro geo-electrical investigation in Gombe town and environs, northeastern Nigeria. J Appl Sci Environ Manage 13: 65–68.

Ates A, Bilim F, Buyuksarac A (2005). Curie point depth investigation of central Anatolia, Turkey. Pure Appl Geophys 162: 357–371.

Aydin I, Karat HI, Kocak A (2005). Curie point depth of Turkey. Geophys J Int 162: 633–640.

Bansal AR, Anand AP (2012). Estimation of depth to the bottom of magnetic sources (DBMS) using modified centroid method from Aeromagnetic data of Central India. In: 9th Biennial International Conference and Exposition on Petroleum Geophysics; Hyderabad, India; p. 343.

Bansal AR, Anand SP, Rajaram M, Rao VK, Dimri VP (2013). Depth to the bottom of magnetic sources (DBMS) from aeromagnetic data of Central India using modified centroid method for fractal distribution of sources. Tectonophysics 603: 155–161.

Bansal AR, Gabriel G, Dimri VP (2010). Power law distribution of susceptibility and density and its relation to seismic properties: an example from the German Continental Deep Drilling Program. J Appl Geophy 72: 123–128.

Bansal AR, Gabriel G, Dimri VP, Krawczyk CM (2011). Estimation of depth to the bottom of magnetic sources by a modified centroid method for fractal distribution of sources: an application to aeromagnetic data in Germany. Geophysics 76: L11–L22.

Benkhelil J, Guiraud M, Ponsard JF, Saugy L (1989). The Bornu-Benue Trough, the Niger Delta and its offshore: tectono-sedimentary reconstruction during the Cretaceous and Tertiary from geophysical data and geology. In: Kogbe CA, editor. Geology of Nigeria. 2nd ed. Ibadan, Nigeria: Abiprint & Pak.

Bhattacharyya BK, Leu LK (1975). Spectral analysis of gravity and magnetic anomalies due to two-dimensional structures. Geophysics 40: 993–1013.

Bhattacharyya BK, Leu LK (1977). Spectral analysis of gravity and magnetic anomalies due to rectangular prismatic bodies. Geophysics 42: 41–50.

Bilim F (2011). Investigation of the Galatian volcanic complex in the northern central Turkey using potential field data. Phys Earth Planet In 185: 36–43.

Blackwell DD, Steele JL (1988). Thermal conductivity of sedimentary rocks: measurements and significance. In Naeser ND, McCulloh TH, editors. Thermal History of Sedimentary Basins. 1st ed. Berlin, Germany: Springer, pp. 13–36.

Blakely RJ (1988). Curie temperature analysis and tectonic implications of aeromagnetic data from Nevada. J Geophy Res 93: 11817–11832.

Blakely RJ (1995). Potential Theory in Gravity and Magnetic Applications. 1st ed. Cambridge, UK: Cambridge University Press.

Bouligand C, Glen JMG, Blakely RJ (2009). Mapping Curie temperature depth in the western United States with a fractal model for crustal magnetization. J Geophy Res 114: 1–25.

Burke KC, Dessauvagie TFJ, Whiteman AJ (1970). Geological history of the Benue Valley and adjacent areas. In Dessauvagie TFJ, Whiteman AJ, editors. African Geology. 1st ed. Ibadan, Nigeria: UNI-IBADAN, pp. 187–205.

Carter JD, Harber W, Tait FA (1963). The geology of parts of Adamawa, Bauchi and Borno provinces in northeastern Nigeria. Bull Geol Surv Nigeria 30: 1–108.

Connard G, Couch R, Gemperle M (1983). Analysis of aeromagnetic measurements from the Cascade Range in the Central Oregon. Geophysics 48: 376–390.

Coulon C, Vida P, Dupuy C, Baudin P, Popoff M, Maluski H, Hermite D (1996). The Mesozoic to early Cenozoic magmatism of the Benue Trough (Nigeria); geochemical evidence for the involvement of the St Helena plume. J Petrol 37: 1341–1358.

Cratchley CR, Louis P, Ajakaiye DE (1984). Geophysical and geological evidence for the Benue-Chad basin cretaceous rift valley system and its tectonic implications. J African Earth Sci 2: 141–150.

Dimri VP (2000). Crustal fractal magnetization. In: Dimri VP, editor. Application of Fractals in Earth Sciences. 1st ed. Oxford, UK: IBH Publishing Co., pp. 89–95.

Dimri VP, Bansal AR, Srivastava RP, Vedanti N (2003). Scaling behaviour of real earth source distribution: Indian case studies. In: Mahadevan TM, Arora BR, Gupta KR, editors. Indian Continental Lithosphere: Emerging Research Trends. Bangalore, India: Geological Society of India, pp. 431–448.

Dolmaz MN, Ustaomer T, Hisarli ZM, Orbay N (2005). Curie point depth variations to infer thermal structure of the crust at the African-Eurasian convergence zone, SW Turkey. Earth Planets Space 57: 373–383.

Eletta BE, Udensi EE (2012). Investigation of the Curie point isotherm from the magnetic fields of the eastern sector of central Nigeria. Geosciences 2: 101–106.

Eze CL, Sunday VN, Ugwu SA, Uko ED, Ngah SA (2011). Mechanical model for Nigerian intraplate earth tremors. Earthzine 1: 1–9.

Fedi M, Quarta T, De Santis A (1997). Inherent power law behavior of magnetic field power spectra from a Spector and Grant ensemble. Geophysics 62: 1143–1150.

Fitton JG (1980). The Benue trough and Cameroon line – A migrating rift system in West Africa. Earth Planet Sc Lett 51: 132–138.

Fitton JG (1981). The West African rift system and its bearing on the origin of continental rifting. In: The African Rift System: A Lunar and Planetary Institute Topical Conference. Houston, TX, USA: NASA, pp. 72–75.

Freeth SJ (1984). How many rifts are there in West Africa? Earth Planet Sc Lett 67: 219–227.

Freeth SJ (1982). Deep structure of the West African Rift system. EOS 63: 1117.

Gregotski ME, Jensen O, Arkani-Hamed J (1991). Fractal stochastic modeling of aeromagnetic data. Geophysics 56: 1706–1715.

Hisarli ZM, Dolmaz MN, Okyar M, Etiz A, Orbay N (2012). Investigation into regional thermal structure of the Trace region, NW Turkey, from aeromagnetic and borehole data. Stud Geophys Geod 56: 269–291.

Kasidi S, Nur A (2012). Curie depth isotherm deduced from spectral analysis of Magnetic data over Sarti and environs of North-Eastern Nigeria. Sch J Biotech 1: 49–56.

Kogbe CA (1983). Geological interpretation of Landsat imageries across central Nigeria. J Africa Earth Sci 1: 313–320.

Kurowska E, Schoeneich K (2010). Geothermal exploration in Nigeria. In: Proceedings of the World Geothermal Congress; Bali, Indonesia, pp. 25–29.

Li CF (2011). An integrated geodynamic model of the Nai-Kai subduction zone and neighbouring regions from geophysical inversion and modelling. J Geodyn 51: 64–80.

Li CF, Shi X, Zhou Z, Li J, Geng J, Chen B (2010). Depths to the magnetic layer bottom in the south China sea area and their tectonic implications. Geophys J Int 182: 1229–1247.

Li CF, Wang J, Lin J, Wang T (2013). Thermal evolution of the North Atlantic lithosphere: new constraints from magnetic anomaly inversion with a fractal magnetization model. Geochemistry Geophysics Geosystems 14: 5078–5105.

Manea M, Manea VC (2011). Curie point depth estimates and correlation with subduction in Mexico. Pure Appl Geophys 168: 1489–1499.

Maus S, Dimri VP (1995). Potential field power spectrum inversion for scaling geology. J Geophy Res 100: 12605–12616.

Maus S, Dimri VP (1996). Depth estimation from the scaling power spectrum of potential field. Geophys J Int 124: 113–120.

Maus S, Gordon D, Fairhead D (1997). Curie temperature depth estimation using a self-similar magnetization model, Geophys J Int 129: 163–168.

Nur A, Ofeogbu CO, Onuha KM (1999). Estimation of the depth to the Curie point isotherm in the upper Benue trough, Nigeria. J Min Geol 35: 53–60.

Nwachukwu JI (1985). Petroleum prospects of Benue Trough, Nigeria. Am Assoc Petr Geol B 69: 601–609.

Nwankwo CN, Ekine AS, Nwosu LI (2009). Estimation of the heat flow variation in the Chad basin Nigeria. J Appl Sci Environ Manage 13: 73–80.

Obande GE, Lawal KM, Ahmed LA (2014). Spectral analysis of aeromagnetic data for geothermal investigation of Wikki Warm Spring, north-east Nigeria. Geothermics 50: 85–90.

Okubo Y, Graft RJ, Hansen RO, Ogawa K, Tsu H (1985). Curie point depths of the Island of Kyushu and surrounding areas, Japan. Geophysics 53: 481–494.

Okubo Y, Matsunaga T (1994). Curie point depth in northeast Japan and its correlation with regional thermal structure and seismicity. J Geophys Res 99: 22363–22371.

Okubo Y, Matsushima J, Correia A (2003). Magnetic spectral analysis in Portugal and its adjacent seas. Phys Chem Earth 28: 511–519.

Okubo Y, Tsu H, Ogawa K (1989). Estimation of Curie point temperature and geothermal structure of island arcs of Japan. Tectonophysics 159: 279–290.

Omanga USA, Abaa SI, Najime T (2001). Radiometric determination of the source of the heat of Wikki Warm Spring in Yankari, Bauchi State of Nigeria. Nigerian J Pure Appl Sci 1: 70–71.

Onuba LO, Chinwuko AI, Onwuemesi AG, Anakwuba EK, Nwokeabia NC (2012). Interpretation of aeromagnetic anomalies over parts of Upper Benue Trough and Southern Chad Basin, Nigeria. Advances in Applied Science Research 3: 1757–1766.

Osazuwa IB, Ajakaiye DE, Verheijen PJT (1981). Analysis of the structure of part of the Upper Benue Rift Valley on the basis of new geophysical data. Earth Evolution Sciences 2: 126–133.

Pilkington M, Gregotski ME, Todoeschuck JP (1994). Using fractal crustal magnetization models in magnetic interpretation: Geophys Prospect 42: 677–692.

Pilkington M, Todoeschuck JP (1990). Stochastic inversion for scaling geology. Geophys J Int 102: 205–217.

Pilkington M, Todoeschuck JP (1993). Fractal magnetization of continental crust. Geophys Res Lett 20: 627–630.

Pilkington M, Todoeschuck JP (2004). Power-law scaling behavior of crustal density and gravity. Geophys Res Lett 31: L09606.

Pilkington M, Todoeschuck JP (1995). Scaling nature of crustal susceptibilities. Geophys Res Lett 22: 779–782.

Qingqing Q, Qingsheng L, Ning Q, Yuanyuan F, Sutao Z, Yao W, Tao Y, Zhenming J (2008). Investigation of Curie point depth in Sulu ultrahigh-pressure metamorphic belt, eastern China. J China Uni Geosci 19: 282–291.

Rajaram M (2007). Depth to Curie temperature. In: Gubbins D, Herrero-Bervera E, editors. Encyclopedia of Geomagnetism and Paleomagnetism. 1st ed. Amsterdam, the Netherlands: Springer, pp. 157–159.

Ravat D, Pignatelli A, Nicolosi I, Chiappini M (2007). A study of spectral methods of estimating the depth to the bottom of magnetic sources from near-surface magnetic anomaly data. Geophys J Int 169: 421–434.

Ross HE, Blakely RJ, Zoback MD (2006). Testing the use of aeromagnetic data for the determination of Curie depth in California. Geophysics 71: 51–59.

Saleh S, Salk M, Pamukcu O (2013). Estimating Curie point depth and heat flow map for northern Red Sea rift of Egypt and its surroundings, from aeromagnetic data. Pure Appl Geophys 170: 863–885.

Salem A, Green C, Ravat D, Singh KH, East P, Fairhead JD, Mogren S, Biegert E (2014). Depth to Curie temperature across the central Red Sea from magnetic data using the de-fractal method. Tectonophysics 624: 75–86.

Salem A, Ushijima K, Elsiraft A, Mizunaga H (2000). Spectral analysis of aeromagnetic data for geothermal reconnaissance of Quseir area, northern Red Sea, Egypt. In: Proceedings of the World Geothermal Congress; Tohoku, Japan. pp. 1669–1674.

Sayed E, Selim I, Aboud E (2013). Application of spectral analysis technique on ground magnetic data to calculate the Curie depth point of eastern shore of the Gulf of Suez, Egypt. Arabian J Geosci 7: 1749–1762.

Sharma PV (2004). Environmental and Engineering Geophysics. 1st ed. Cambridge, UK: Cambridge University Press.

Shuey RT, Schellinger DK, Tripp AC, Alley LB (1977). Curie depth determination from aeromagnetic spectra. Geophys J Roy Astr Soc 50: 75–101.

Silva JBC (1986) Reduction to the pole as an inverse problem and its application to low-latitude anomalies. Geophysics 51: 369–382.

Smith RB, Shuey RT, Pelton JR, Bailey JP (1977). Yellowstone hot spot: contemporary tectonics and properties from earthquakes and magnetic data. J Geophys Res 82: 3665–3676.

Spector A, Grant FS (1970). Statistical models for interpreting aeromagnetic data. Geophysics 35: 293–302.

Stacey FD (1977). Physics of the Earth. 2nd ed. New York, NY, USA: John Wiley & Sons.

Stampolidis A, Tsokas G (2002). Curie point depths of Macedonia and Thrace, N. Greece. Pure Appl Geophys 159: 1–13.

Starostenko VI, Dolmaz MN, Kutas RI, Rusakov OM, Oksum E, Hisarli ZM, Okyar M, Kalyoncuoghu UY, Tutunsatar HE, Legostaeva OV (2014). Thermal structure of the crust in the Black Sea: Comparative analysis of magnetic and heat flow data. Marine Geophys Res 35: 345–359.

Tanaka A, Okubo Y, Matsubayashi O (1999). Curie point depth based on spectrum analysis of the magnetic anomaly data in East and Southeast Asia. Tectonophysics 306: 461–470.

Trifonova P, Zheler Z, Petrova T, Bojadgieva K (2009). Curie point depths of the Bulgarian territory inferred from geomagnetic observations and its correlation with regional thermal structure and seismicity. Tectonophysics 473: 362–374.

Tsokas G, Hansen RO, Fyticas M (1998) Curie point depth of the Island of Crete (Greece). Pure Appl Geophys 159: 1–13.

Ubaru JI (2000). Review of Illegal Activities in Yankari National Park (1991–1999). Report Submitted to Savanna Conservation Nigeria. Kaduna, Nigeria: Savanna Conservation.

Zaborski PM (1998). A review of the Cretaceous system in Nigeria, Africa. Geosciences Review 5: 385–483.